processes

MDPI

Review

Biomass Pyrolysis: Recent Advances in Characterisation and Energy Utilisation

Hamid Reza Nasriani * and Maryam Nasiri Ghiri

School of Engineering & Computing, University of Lancashire, Preston PR1 2HE, UK
* Correspondence: hrnasriani@lancashire.ac.uk

Abstract

Biomass pyrolysis has emerged as a flexible platform for converting low-value residues into higher-value energy carriers (bio-oil, biochar and gas) and carbon-rich materials, with realistic potential for negative emissions when biochar is deployed in long-lived sinks. Over the last decade, three developments have driven the field forward: first, a finer mechanistic understanding of devolatilization and secondary reactions; second, major improvements in analytical techniques for characterising feedstocks and products; and third, more rigorous techno-economic and life-cycle assessments that place pyrolysis in a broader energy-system context. Recent experimental work on forestry and agro-industrial residues has clarified how biomass composition, ash chemistry and operating conditions jointly govern product yields, energy content and stability. Parallel advances in GC×GC–MS, high-resolution mass spectrometry, NMR and thermogravimetric methods have shifted the discussion from bulk "bio-oil" and "char" to families of molecules and well-defined structural domains, which can be deliberately targeted by reactor and catalyst design. Data-driven models, ranging from support vector machines applied to TGA curves to ANFIS and random forests for yield prediction, are now accurate enough to support process screening and multi-objective optimisation. At the system level, commercial fast pyrolysis biorefineries report overall useful energy efficiencies on the order of 80–86%, while slow pyrolysis configurations centred on biochar can be economically viable when carbon storage and co-products are appropriately valued. Thermodynamic analyses confirm that indirect gasification via fast-pyrolysis oil sacrifices some energy and exergy efficiency relative to direct solid-biomass gasification but may offer logistical and integration advantages. This review synthesises recent work on (i) feedstock and process characterisation; (ii) state-of-the-art analytical methods for bio-oil, biochar and gas; (iii) modelling and machine-learning tools; and (iv) energy-system deployment of pyrolysis products. Throughout, the emphasis is on how characterisation and modelling inform concrete design choices and on the trade-offs that arise when pyrolysis is considered as part of a wider decarbonisation portfolio. By integrating laboratory-scale characterisation with system-level modelling, this review aligns biomass pyrolysis with several United Nations Sustainable Development Goals (SDGs). The optimisation of thermochemical conversion pathways for forestry and agro-industrial residues directly supports SDG 7 (Affordable and Clean Energy) by enhancing the efficiency of bio-oil and syngas production. Furthermore, the deployment of biochar as a stable carbon sink for negative emissions and soil amendment addresses SDG 13 (Climate Action) and SDG 15 (Life on Land). By converting low-value waste streams into high-value energy carriers and chemicals within a circular bioeconomy framework, the research further contributes to SDG 12 (Responsible Consumption and Production) and SDG 9 (Industry, Innovation and Infrastructure).

Academic Editors: Leandro Ayarde-Henríquez and Eduardo Chamorro

Received: 9 March 2026
Revised: 13 April 2026
Accepted: 14 April 2026
Published: 21 April 2026

Keywords: biomass pyrolysis; fast pyrolysis bio-oil; biochar stability; thermogravimetric analysis; machine learning; techno-economic analysis; life cycle assessment; deoxygenation; lignocellulosic residues; carbon-negative emissions

1. Introduction

The global energy transition is not unfolding along a single technological pathway but through a patchwork of incremental improvements in existing systems and the parallel development of genuinely low-carbon options. Work on optimising natural-gas production and transport has helped to stabilise energy supply in the short term while carbon-intensive fuels are phased down [1–6]. In parallel, detailed studies of unconventional resources, including tight and shale gas, have shown both the potential and the limitations of using these reservoirs as bridging options in transition scenarios [7–9].

At the same time, attention has shifted decisively towards carbon-lean vectors and carbon-management technologies. Hydrogen produced from waste streams, including mixed plastics via pyrolysis and in-line reforming with carefully integrated heat management, is now viewed as one way to decarbonise hard-to-electrify sectors while tackling resource inefficiencies in the waste system [9–13]. In parallel, carbon capture, utilisation and storage (CCUS) concepts are being developed to deal explicitly with the stock of greenhouse gases already in the atmosphere [14–19]. Together, these strands underscore a broader point: thermochemical processing and sorbent-based separations are likely to remain central tools in any credible route to net-zero and net-negative emissions.

Within this family of thermochemical options, biomass pyrolysis occupies a distinctive position. Thermochemical routes for biomass conversion—combustion, gasification and pyrolysis—offer different balances between simplicity, efficiency and product flexibility. Combustion maximises immediate heat release for heat and power; gasification targets a gaseous intermediate for downstream synthesis; pyrolysis redistributes carbon among condensable vapours (bio-oil), solid carbonaceous residue (biochar) and non-condensable gases under oxygen-deficient conditions [20–23]. By adjusting temperature, heating rate and vapour residence time, this distribution can be tuned towards short-lived energy carriers (bio-oil and gas) or longer-lived carbon sinks (biochar), which is why pyrolysis features prominently in scenarios for carbon-negative energy systems [20,24–27]. Fast pyrolysis, typically at 450–550 °C with very high heating rates and vapour residence times below a few seconds, is designed to maximise liquid yields, whereas slow pyrolysis with lower heating rates and longer residence times favours char formation and structural rearrangement towards more aromatic, stable solids [21,26,28–30]. Figure 1 conceptually maps these regimes and their characteristic product-yield envelopes.

Several comprehensive reviews have already covered fundamental aspects of biomass pyrolysis, including classical process overviews and reactor technologies, detailed discussions of reaction mechanisms, and broad surveys of fast pyrolysis and product upgrading [20–23,25–27]. Building on this foundation, the present article is not intended as another general survey of all pyrolysis work. Instead, it focuses on four inter-linked themes that have developed rapidly over roughly the last decade: (i) the way feedstock properties and thermogravimetric behaviour inform process design and control; (ii) advances in analytical characterisation of bio-oil, biochar and pyrolysis gas at molecular and microstructural levels; (iii) the emergence of modelling and machine-learning tools that link operating conditions and biomass composition to yields, quality metrics and stability; and (iv) the integration of these insights into energy-system deployment, including techno-economic analysis (TEA) and life-cycle assessment (LCA) of fast- and slow-pyrolysis pathways.

https://doi.org/10.3390/pr14081321

The scope of the review is deliberately confined to the pyrolysis of solid lignocellulosic biomass and its direct co-feeds, processed in slow, intermediate or fast regimes. We do not attempt to cover hydrothermal liquefaction, conventional combustion, or gasification except where they provide context for comparing energy and exergy performance. Likewise, we touch on co-pyrolysis with plastics or other wastes only insofar as it informs understanding of biomass-derived product character. By structuring the review from fundamentals (Section 2) through feedstock and product characterisation (Sections 3 and 4), reactor concepts (Section 5), energy utilisation (Section 6), modelling (Section 7) and TEA/LCA (Section 8), we aim to provide a measurement-driven, system-aware perspective that links laboratory-scale characterisation with deployable biomass-pyrolysis options in decarbonisation strategies.

Thermochemical routes for biomass conversion—combustion, gasification, and pyrolysis—offer different balances among simplicity, efficiency, and product flexibility [20–23]. Combustion maximises immediate heat release; gasification targets gaseous intermediates for fuel synthesis; pyrolysis distributes carbon among gas, liquid and solid phases under oxygen-deficient conditions. That distribution can be tuned towards shorter-lived energy carriers (bio-oil and gas) or longer-lived carbon sinks (biochar), which is why pyrolysis increasingly appears in discussions of negative-emission and circular bioeconomy [20,25–27].

Fast pyrolysis, usually conducted at 400–650 °C with very high heating rates and vapour residence times below a few seconds, is optimised for condensable vapours that can be recovered as a liquid "bio-oil" [21,26,28–31]. Slow pyrolysis, with heating rates of order 1–10 °C s^{-1} and much longer solid residence times, favours char formation and structural rearrangement towards more aromatic, stable solids. Figure 1 conceptually maps these regimes, indicating typical operating windows and product-yield envelopes. Intermediate and staged configurations blur the classical "slow vs. fast" dichotomy and are increasingly used to manage secondary reactions. This figure presents the average particle size used in different processes; however, biomass feedstocks can exhibit wide variation in particle size, which may influence heat transfer efficiency and reaction surface area during pyrolysis.

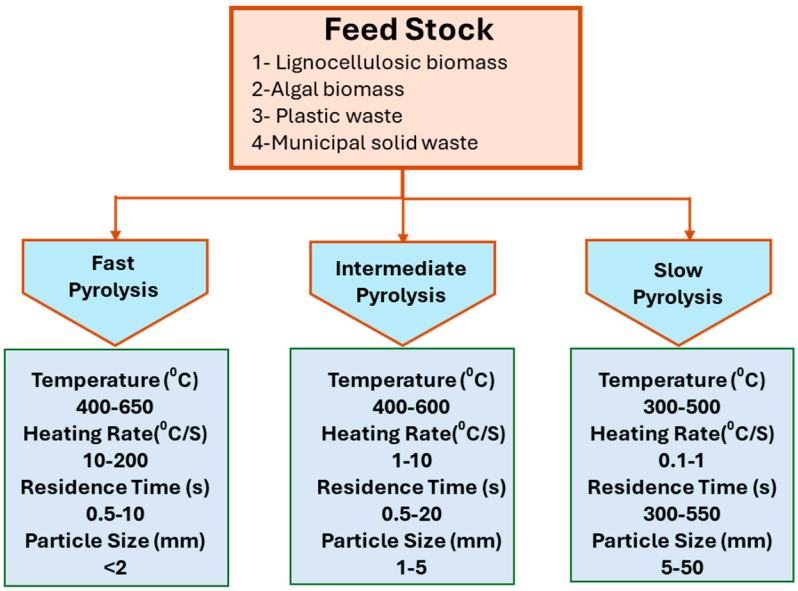

Figure 1. Conceptual map of biomass pyrolysis regimes (slow, intermediate, and fast) showing typical temperature, heating rate and vapour-residence windows and approximate product-yield envelopes.

In parallel with process developments, the analytic side of pyrolysis has advanced markedly. It is now routine to combine proximate and ultimate analysis with TGA/DTG,

detailed gas chromatography, multi-dimensional separations and high-resolution MS/NMR to build a multi-scale picture of how a given feedstock responds to a specific operating window [25,32–37]. These techniques, summarised in Table 1, have turned characterisation from a post hoc exercise into a central design tool. The sections that follow link feedstock properties, process conditions, product characterisation and energy utilisation, drawing out implications for future deployment.

Table 1. Overview of analytical methods for bio-oil characterisation: technique, target analytes, strengths, limitations, and typical use cases.

Techniques	Target Analysis	Disadvantages	Advantages
Gas Chromatography **1- Mass spectrometric detector (GC-MS)** **2- Flame ionisation detector (GC-FID)**	Chemical composition & chemical structure of compounds (pyrolysis liquids)	Insufficient chromatographic resolution peak coelution unavailability of mass spectra of some bio-oil components in MS libraries unable to characterise the non-volatile compounds	Acceptable price wide availability
Pyrolysis Gas Chromatograph–Mass Spectrometry (Py GC-MS) **1- Online pyrolysis: the pyrolysis products are directly introduced into the injector of the gas chromatograph**	Studying the process of biomass pyrolysis and its products in the lab-scale	Online pyrolysis: discrimination of high-molecular components, poor chromatographic behaviour of polar compounds, deterioration of GC columns due to the presence of non-volatile components.	
2- Offline pyrolyses: pyrolysis products are captured on the sorbent and subsequently eluted with the solvent		Offline pyrolysis: long sampling time for high-molecular compounds	Eliminates the memory effects and column deterioration and enables further sample treatment (e.g., derivatization) before the analysis
Two-dimensional gas chromatography (GC × GC).	By separating on two capillary columns, analyse extremely complex mixtures	High purchase price limitation to the compounds with boiling points up to ~400 °C	achieving an extended theoretical peak capacity, enhanced chromatographic resolution significantly higher number of detected components in comparison to the conventional GC-MS technique
Liquid Chromatography (LC) **1- Adsorption chromatography (LSC)** **2- Gel permeation chromatography** **3- High-performance liquid chromatography with UV**	Separate, identify, and quantify compounds dissolved in a liquid sample	Worse separation ability than gas chromatography *Unamenable to some heavy fractions of bio-oil	Ability to analyse volatile components and non-volatile substances
High-resolution mass spectrometry (HRMS)	Determine the feedstock and pyrolysis process conditions to produce bio-oils with the desired properties	Discrimination of some compounds in the ionisation process	Ability to analyse non-volatile, high-molecular components
Nuclear magnetic resonance (NMR).	*Determine the percentage of different carbon and hydrogen atoms in the sample, *Provide information about the concentrations of different functionalities in bio-oils *Estimating the alkyl chain length of the alkanes present, or the degree of their branching	*Relatively low sensitivity as compared to other spectroscopic techniques *Trace and ultra-trace level quantitation are always represented by poor limits of detection, that is, several orders of magnitude poorer than mass spectrometry or emission/absorption/fluorescence-based techniques	Characterise almost the entire bio-oil sample, including the high-molecular components
Fourier Transform infrared spectroscopy (FTIR)	Characterisation of the entire bio-oil sample, regardless of the volatility of the compounds present	The methanol stabilisation reduced viscosity and positively affected the stability of the bio-oil samples, which resulted in a reduction in the functional group changes in FTIR spectra	Simple, cheap and fast

2. Fundamentals of Biomass Pyrolysis

2.1. Biomass Constituents and Intrinsic Reactivity

Lignocellulosic biomass is typically composed of 30–60% cellulose, 20–35% hemicellulose and 15–30% lignin, plus extractives and ash [21–23,25,38]. These biopolymers decompose over overlapping but distinct temperature intervals: hemicellulose around 200–350 °C, cellulose 300–380 °C and lignin over a much broader range up to 600–700 °C. Figure 2 compares DTG curves for model cellulose, hemicellulose and lignin with a representative whole-biomass sample, illustrating the characteristic peaks associated with each component.

Cellulose tends to depolymerise into anhydrosugars and low-molecular-weight oxygenates; hemicellulose, being more branched and heteroatom-rich, typically generates more permanent gas and small acids; lignin decomposes more slowly into phenolic vapours and char [23,28,31,38–40]. The relative proportions of these components therefore influence both the amount of char and the phenolic richness of the vapour phase.

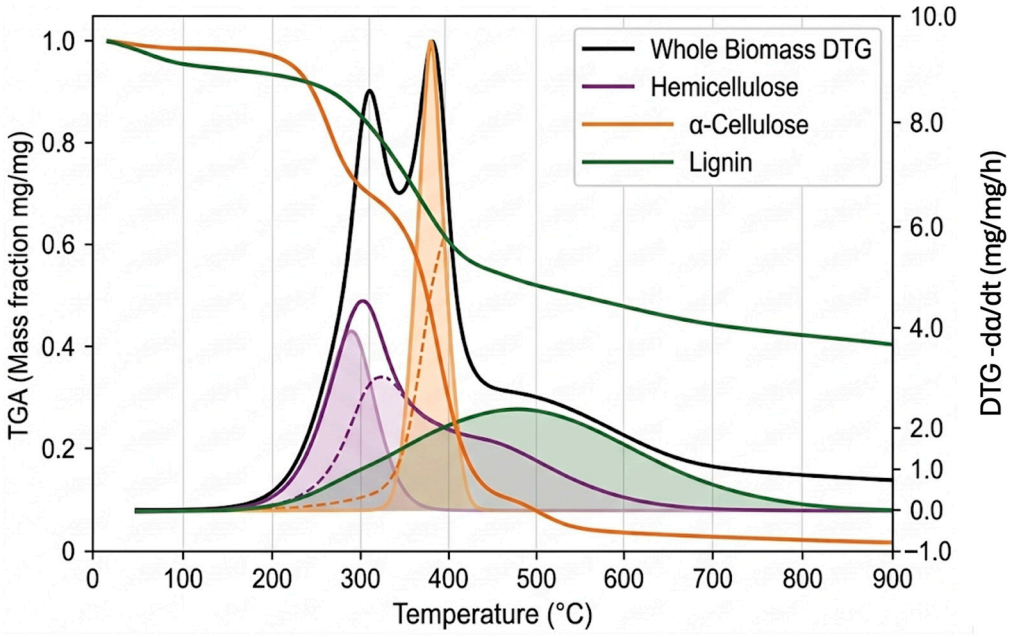

Figure 2. DTG curves for model cellulose, hemicellulose and lignin with a representative whole-biomass sample, illustrating the characteristic peaks associated with each component.

2.2. Operating Regimes and Product Distributions

The distinction between slow, intermediate and fast pyrolysis is fundamentally kinetic: it hinges on the relative rates of heat transfer, primary devolatilisation and secondary cracking/condensation. Under slow conditions, char yields of 25–35 wt.% with relatively modest liquid yields are typical; under optimised fast-pyrolysis conditions, liquids can reach 65–75 wt.% of dry feed for clean woody biomass, with char around 10–20 wt.% and gas 10–25 wt.% [20,21,26–28,41–45]. Representative ranges for different regimes and feedstocks are collated in Table 2.

Fixed-bed work on residual forest and agro-forestry biomass confirms familiar but important trends: as peak temperature is raised from about 350 to 550 °C at moderate heating rates, char yield decreases while its fixed-carbon and ash fractions increase; H/C and O/C ratios drop substantially, indicating progressive aromatisation and deoxygenation. Simultaneously, the permanent gas fraction becomes richer in CO, H_2 and CH_4, and the liquid fraction shifts towards lighter oxygenates at the expense of heavier oligomers. Particle size exerts a strong influence, with finer particles improving liquid yield by reducing intra-particle residence times and secondary cracking.

Table 2. Representative proximate and ultimate analyses for different biomass types, with typical product yields and char higher heating value (HHV) at standard fast and slow pyrolysis conditions.

Biomass	Temp (°C)	Heating Rate (C/min)	Process	Bio-Oil Yield (wt.%)	Gas-Yield (wt.%)	Char Yield (wt.%)	HHV (MJ/kg)	Ref
Acid-treated rice husk	300–600 (427)	10	slow	35.5		49.2	14.6	[46]
Spent coffee waste	400–800 (500)	3–15 (10)	slow			30	22.6	[46]
Banana pseudostem	470–540 (500)		fast	39.4			5.35	[46]
Eucalyptus and LDEP	300–600 (524)			17.3				[46]
Tomato peel waste	450–650 (600)	5–25	slow	40			22.5	[46]
Palm shell	400–600 (500)		fast	60				[46]
Sal wood sawdust	500	80	fast	46			36.1	[46]
salicornia	600–800 (700)	15	slow	18–22.7		36.7–45.7	10.2–17.6	[46]
Sewage sludge	300–700 (300)			72–52				[46]
coffee grounds, and cow manure	350–750	5–10	slow	28–61	6–42	23–55		[47]
Neem seed-based de-oiled cake	400–700 (523)	25		47.0883		70.21	26.73	[48]
waste palm kernel cake	550	1000	fast	60				[49]
hardwood	500	10–20 (20)	slow	42.4	33.4	24.2		[50]
pressed mustard oil cake	500	10–20 (20)	slow	40.5	36.3	23.2		[50]
corncob	500	10–20 (20)	slow	43.9	33.3	22.8		[50]
Hardwood + pressed mustard oil cake + corncob	500	10–20 (20)	slow	40.1	37.4	22.7		[50]
Mahua and neem de-oiled seed	160–530 (450)	20	slow	42.6		40.1		[51]
Medium-density fibreboard	1046	10	intermediate	16.75	27.2	25	21.28	[52]
Brewery spent grains	1046	10	intermediate	36.02	16.23	22.5	21.28	[52]
Post-extraction soybean meal	1046	10	intermediate	20.88	16.15	32.4	21.28	[52]
Neem Seed (NS), Pigeon Pea husk (PP), Yellow Pea husk (YP), Ground Nut shell (GN), Soyabean Straw (SS), Wheat Straw (WS), Sawdust (SD)	500	10	intermediate	47.5, 30, 40, 30, 20.5, 34.5, 42.5	29.5, 32.5, 30, 30, 40.5, 24.5, 24.5	32, 32.5, 30, 37, 40, 40, 27.5		[53]

3. Feedstock Characterisation and Process Implications

3.1. Proximate/Ultimate Analysis and Mineral Effects

Proximate and ultimate analyses remain the starting point for correlating feedstock with pyrolysis behaviour. Table 2 presents representative proximate/ultimate data for softwood, hardwood, and an agro-residue, alongside indicative product yields and char heating values under standard conditions. Higher volatile matter typically correlates with higher combined liquid and gas yields, while higher fixed-carbon and lignin content favour char.

Ash content and composition are equally important. Even at modest levels, alkali and alkaline-earth metals catalyse dehydration, decarboxylation, and cracking, often depressing liquid yields and enriching gas in CO and CO_2. In a comparative study of white ash, switchgrass and corn stover, more than half of the inlet carbon remained in the char at moderate temperatures, and the combustible gas fraction ($CO + H_2 + CH_4$) varied between roughly 50 and 70 vol.% depending largely on mineral speciation.

3.2. Thermogravimetric Analysis and Kinetic Interpretation

Thermogravimetric analysis is now the default tool for probing devolatilisation behaviour. DTG curves, as sketched in Figure 2, can be deconvoluted into pseudo-

component peaks to estimate apparent kinetic parameters for hemicellulose, cellulose and lignin in a given biomass. Biagini and Tognotti proposed a generalised procedure to infer chemical-component fractions directly from TGA data, and validated it on a wide range of biomass types, effectively linking simple thermal tests to compositional fingerprints [39].

Awad and co-workers took a more pragmatic route: they carried out pyrolysis experiments on several organic wastes across a broad temperature range and then built regression models relating biochar and bio-oil yields and their heating values to both temperature and compositional descriptors (volatiles, ash, elemental ratios). Those models were then embedded in a multi-response desirability framework to identify operating windows that jointly maximise desirable responses (for example, high char HHV and acceptable oil yield), an approach that anticipates the kind of multi-objective optimisation discussed later in Section 7.

3.3. Data-Driven Links Between Feedstock and Products

Machine learning adds another layer of insight. Li and co-workers compiled nearly 250 data points from the literature and trained GA- and PSO-optimised ANFIS models to predict bio-oil yield from process conditions and biomass composition, achieving high coefficients of determination and low errors. Sensitivity analysis ranked temperature, heating rate and carbon content as the dominant variables, with ash and nitrogen exerting subtler effects.

Zhu and co-workers, working on biochar, used random forests to predict both char yield and carbon content from compositional and operating variables across a large dataset, and found that ash, lignin and temperature were key drivers. Yin and co-workers approached the problem from a different angle, using TGA curves as input features to a support vector machine classifier that automatically recognises biomass type and growing conditions in tobacco; classification accuracies above 90% suggest that TGA-based "fingerprints" could be used more broadly for feedstock screening. More recent studies have extended such approaches to predicting bio-oil properties directly from feedstock composition and operating conditions.

These studies, summarised in Table 3, highlight that feedstock characterisation and process conditions together define a high-dimensional design space, and that data-driven tools are increasingly capable of navigating it.

Table 3. Machine learning and ANN applications in bio-oil yield and quality forecasting.

Input Variables	Output	Methods	Performance	Key Insights	ref
Temperature (HT), Heating rate (HR), Feedstock particle size (PS)	*Bio-oil yield *quality of bio-oil	ANN	$R^2 > 0.9960$	ANN and SVM were used, with ANN having the best performance Provided intricate relationships between process variables and bio-oil properties 90% of the data was used for training the ANN model 3 neurons in the input layer, 9 in the hidden layer, and 1 in the output layer Create a predictive model for bio-oil properties	[54]
Biomass Type Temperature, HR, Reaction time (RT)	Bio-oil yield	DNN	R^2~0.931 AAE~3.583 RMSE~4.57	Deep Neural Networks (DNN) and Lightweight Gradient Boosting Machines. Dataset consisting of 122 data points. Dataset divided into training and testing sets at a ratio of 3:1 Integrates the pyrolysis data of the three major components of biomass (cellulose, hemicellulose, and lignin), both individually and in mixtures, Incorporation of biomass component data significantly improves the prediction accuracy of co-pyrolysis bio-oil yield	[55]
VM (%) Fixed carbon (FC) (%) Ash (%)	Biochar yield biochar HHV	*RF regress (biochar yield)	R^2~0.86 (biochar yield)	*Dataset comprising 423 observations from 44 different biomasses from the literature.	[56]

MC (%) Carbon (C) (%) Hydrogen (H) (%) Oxygen (O) (%) Nitrogen (N) (%) Pyrolysis Temperature (PT) HR RT		*XGB regress (biochar HHV)	R^2~0.87 (biochar HHV)	Two distinct datasets were prepared: one for predicting biochar yield and the other for predicting biochar HHV. Pyrolysis temperature and ash content of biomass were identified as the most influential features for the prediction of both yield and HHV of biochar.	
HR (°C/min), PT, C (%), Ash (%), FC (%), Volatile (V (%)), H (%), N (%), O (%), HT (°C), PS (mm), Nitrogen flow rate (NFR-L/min), Higher heating value (HHV-kJ/kg)	Bio-oil yield	Gradient boosting method	R^2~0.89 RMSE~2.39	Different models, such as multi-linear regression, gradient boosting, random forest, and decision tree, have been trained on the dataset Bio-oil yield during the pyrolysis of lignocellulosic biomass does not follow linear relations with the considered pyrolysis parameters, namely, HR and PT *Bio-oil yield was significantly influenced by the HR and total C	[57]
Proximate analysis, Ultimate analysis of the agricultural feedstock, Pyrolysis reaction conditions	Bio-oil yield	Categorical boost model	RMSE~2.9 R^2~93.2	*387 data points are gathered from various literature sources *Eight different machine-learning algorithms were investigated *Identify the input variables that had the greatest impact on bio-oil production In the pyrolysis of agricultural waste, hydrogen content is one of the most crucial parameters for maximising bio-oil yield	[58]
PT (°C), C (%) O (%) H (%) N (%) HR (°C/min) Moisture content-MC (%) V (%) FC (%) Sulfur (S-%) Flow rate (mL/min)	Nitrogen-containing yields	ANN	R^2~0.9357. RMSE ≈ 3.4	*Optimising the pyrolysis process and achieving its high-value conversion * Utilising a dataset including 195 sets of experimental data * Try different types of ML methods including support vector regression machine (SVR), random forest (RF) and neural network *Pyrolysis temperature, heating rate, and feedstock nitrogen content are the most influential factors controlling nitrogenous product formation. Based on model outputs and mechanistic interpretation, practical measures to minimise nitrogen-containing compounds	[59]
Cellulose Ligni Hemi-cellulose C (%), H (%), N (%), S (%) V (%), O (%), Ash (%), FC (%), MC (%), Protective gas flow rate, Pyrolysis time (PT), Protective gas Biochore (%), Bio-oil Non-condensable gas (%)	Nitrogen-containing yield	GBDT model	MSE~10.04 and R^2~0.92	*Dataset containing 468 samples *Investigating algorithms are random forest, GBDT, SVR, and ANN. *The content of volatiles, fixed carbon, and sulfur significantly affects the yield of pyrolysis products *This model assists researchers and engineers in optimising pyrolysis process parameters to enhance product yield and quality	[60]
HR, plastic-type, biomass-type, temperature, PS	Bio-oil yield quantitatively (amount) and qualitatively (composition)	GBR	$R^2 > 0.97$	*Investigates the impacts of feedstock composition and operating conditions in pyrolysis (individual feedstock) and co-pyrolysis (biomass and plastic wastes *Reveals that synergistic effects, specifically improved yields and optimised temperature, exist in the co-pyrolysis of biomass and plastic wastes compared to individual feedstock *Different ML methods are explored, including random forest, gradient boosting regressor, and XGBoost *Key factors contributing to yield include plastic content (18%) and biomass type (13%). *Introducing the optimal bio-oil yield and quality conditions using co-pyrolysis of wood, bagasse and plastic wastes	[61]

Cellulose (%), Lignin (%), Hemicellulose (%), PT (°C), HR (°C/min)	Bio-oil, Biochar, gas yield	XGB	$R^2 > 0.9$	*Dataset of 273 experiments *Evaluating five machine learning models, including multiple linear regression (MLR), k-nearest neighbours regression (kNN), support vector regression (SVR), random forest regression (RFR), and XGBoost regression (XGB) *Identified key parameters influencing product yields	[62]
V (%) FC (%) MC (%) Ash (%) C (%) H (%) N (%) O (%) Gas yield (GY)-(%) Bio-oil yield (BOY)-(%) Water yield (WY)-(%) Carbon monoxide (CO)-(%) Char yield (CY)-(%) H_2 (%) Methane (CH_4)-(%) C-bio-oil (CBO)-(%) H-bio-oil (HBO)-(%) N-bio-oil (NBO)-(%) O-bio-oil (OBO)-(%)		XGB	R^2~0.89	*This study predicts output products, optimises the process, and investigates process feasibility *Examining random forest, artificial neural network, ANN, and eXtreme gradient boosting ensemble tree, XGBoost *Ability of this model to predict the production of upgraded bio-oil products from a broad range of biomass species, and calculate the energy requirements, electricity generated, and CO_2 emissions by specifying the biomass characteristics and pyrolysis temperature only	[63]
VF, FC, MC, Ash, C, H, N, O, Cellulose, Lignin, Hemi-cellulose, ps, metal, loading, si/Al, weak, medium, and strong acid, S_{BET}, V_{total}, V_{micro}, V_{meso}, type, PT, catalyst particle size (CPS), Flow rate, catalyst-to-biomass ratio (C/B)	Yields of bio-BTX (biomass-derived benzene, toluene and xylene) and light olefins	RF	$R^2 > 0.91$	*Utilising random forest (RF), gradient boosting decision tree and extreme gradient boosting algorithms * Show the effective parameters for different yields *Specify the influence of input features on the output targets *Provide a feasible reference for the selection of parameters and prediction of target product yields in zeolite-catalysed biomass pyrolysis	[64]

4. Product Characterisation

4.1. Biochar: Structure, Stability and Functional Properties

Biochar has shifted from being an inconvenient solid residue to a central product in its own right. Basic descriptors—proximate and ultimate analysis, HHV, H/C and O/C—are now routinely complemented by BET surface area, pore-size distribution, FTIR, Raman and sometimes XRD [21,25,65–68].

Figure 3 plots H/C versus O/C for a set of biomass samples and their chars produced at, for example, 350, 450 and 550 °C. The trajectories show a consistent movement towards lower H/C and O/C with increasing severity, approaching domains associated with more aromatic and graphitic structures. Many practitioners use empirical criteria such as H/C_org < 0.4 and O/C < 0.2–0.3 as proxies for long-term stability in soil, extrapolating from natural charcoal and black-carbon data.

Machine-learning studies refine this picture by quantifying variable importance. When a large set of literature biochars is analysed, feedstock composition (particularly oxygen-rich fractions and minerals) largely controls O/C, while process parameters (temperature, residence time) dominate H/C and aromaticity. This is important for design: some feedstocks simply cannot yield highly stable chars without extreme and possibly uneconomic process conditions.

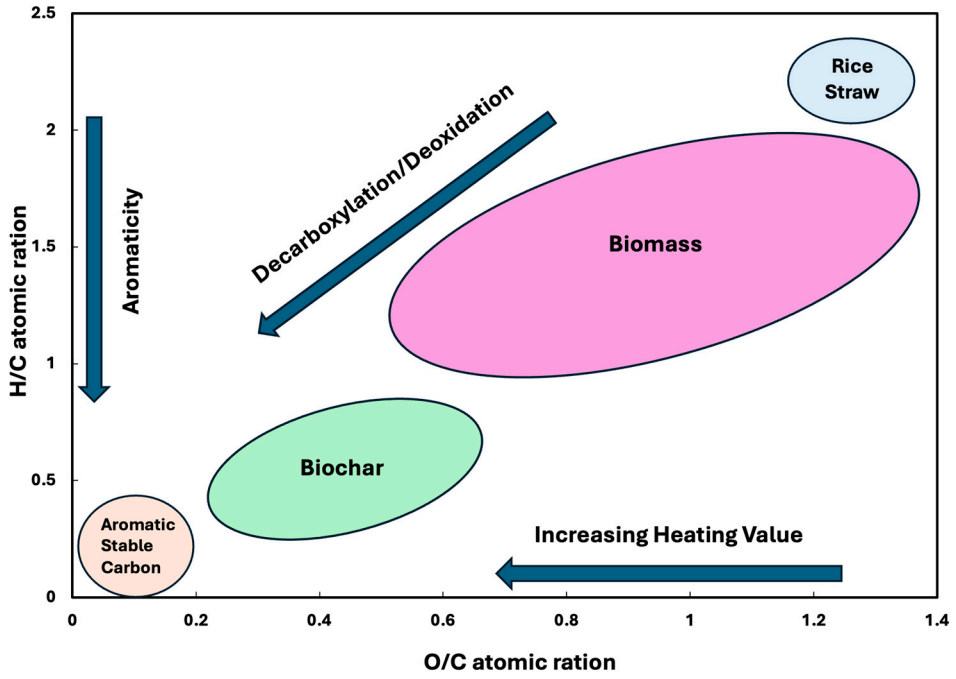

Figure 3. H/C vs. O/C for several biomass feedstocks and their biochars at different temperatures, illustrating trajectories towards more aromatic and stable domains [69,70].

Functionally, the properties that matter depend on the application. For energy use, HHV, ash fusion and grindability are critical; for soil applications, cation exchange capacity, surface oxygen groups and pore structure govern nutrient and water interactions; for adsorption and catalysis, surface area, pore architecture and specific functionalities dominate [20,65–68,71]. Tables 1 and 2 can be used together to link typical char properties with the feedstock and conditions that produced them.

4.2. Bio-Oil: Bulk Properties, Analytical Toolbox and Upgrading

Raw fast-pyrolysis oil is a metastable, acidic, oxygen-rich emulsion. Typical oxygen contents are 35–50 wt.%, water contents 15–30 wt.%, pH around 2–3 and HHVs roughly at 16–20 MJ kg^{-1} [23,26–28,34,37]. The oil contains hundreds to thousands of identifiable compounds—light oxygenates (acids, aldehydes, ketones), phenolics, furans, anhydrosugars and heavier oligomeric material—and tends to age via condensation and polymerisation reactions that increase viscosity and may cause phase separation [30,32–34,72]. Figure 4 presents a simplified compositional breakdown of a representative oil, distinguishing water, light oxygenates, phenolics, sugars/oligomers and heavy residues. The subsequent bar graph (right) details the upgrading process, showing the specific yield of monomeric compounds (in g/kg PO) such as phenols, guaiacols, and catechols. This comparison highlights the efficacy of various palladium-based catalysts (Pd/SiO_2, Pd/Nb_2O_5, and Fe-modified variants) in shifting the chemical profile toward high-value aromatic and oxygenated intermediates.

The current analytical toolbox for such complex liquids is summarised in Table 1. Karl Fischer titration, elemental analysis and basic distillation or simulated distillation establish water content, CHONS composition and volatility profiles. GC/MS and GC×GC–MS resolve a large fraction of light and medium-boiling oxygenates and aromatics, while HPLC and UPLC target polar and high-molecular-weight fractions [29,34–37]. High-resolution mass spectrometry (Orbitrap, FT-ICR) maps thousands of individual formulae, often represented as van Krevelen clouds, and NMR (^1H, ^{13}C, 2D methods) quantifies functional-group distributions [45,73,74].

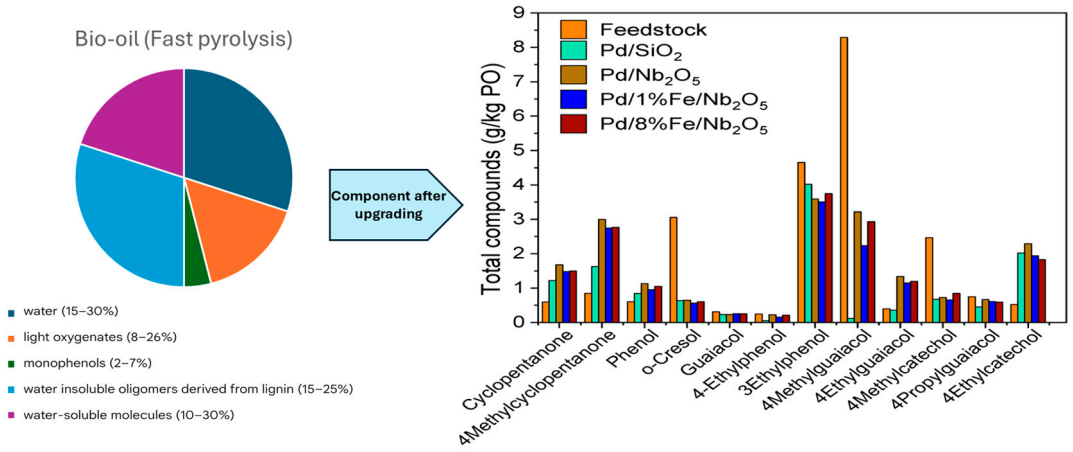

Figure 4. Comparison of bio-oil components and the effect of palladium-based catalysts on total compound yield.

Sample preparation (solvent choice, derivatisation, and fractionation) and chromatographic conditions can strongly bias the apparent composition, which has motivated moves towards more standardised protocols, especially for stability testing.

From an energy-utilisation standpoint, the central challenge is to convert this chemically mixed and unstable liquid into something that behaves more like a conventional fuel. Strategies include ex situ hydrodeoxygenation, catalytic cracking and in situ catalytic fast pyrolysis using zeolites and metal oxides. Co-pyrolysis with hydrogen-rich plastics, followed by catalytic or plasma upgrading, has also shown promise in increasing monocyclic aromatics while suppressing heavy polycyclic aromatics and oxygenates.

4.3. Pyrolysis Gas and Syngas Quality

The non-condensable gas fraction—mainly CO_2, CO, H_2, CH_4 and light hydrocarbons—plays a dual role as an energy vector and a process-internal heat source. Typical compositions and lower heating values for different regimes and temperatures are collected in Table 2. As temperature and severity increase, gas generally becomes richer in H_2 and CH_4, raising its heating value and making it more attractive for engines or microturbines rather than simple flaring.

Gas analytics, however, often lag behind those for liquids and solids. Many studies report only aggregate CO, CO_2, CH_4 and "light hydrocarbons", with limited tar speciation. Where engines, turbines or synthesis are envisaged, more detailed GC and tar characterisation is required, alongside measurements of trace contaminants (NH_3, H_2S, HCN) and particulates. The use of biochar and heavy fractions as internal sorbents and catalysts for gas cleanup, discussed later in Section 6.3, illustrates how product characterisation feeds directly into process integration.

5. Reactor Concepts and Process Intensification

Classical reactor types for pyrolysis—fixed beds, bubbling and circulating fluidised beds, ablative reactors, auger and screw reactors—each present characteristic trade-offs in terms of heat transfer, residence time control and scalability. Figure 5 sketches a representative fast-pyrolysis biorefinery flowsheet based on a fluidised-bed reactor, coupled to cyclones, condensers and a char/gas combustor.

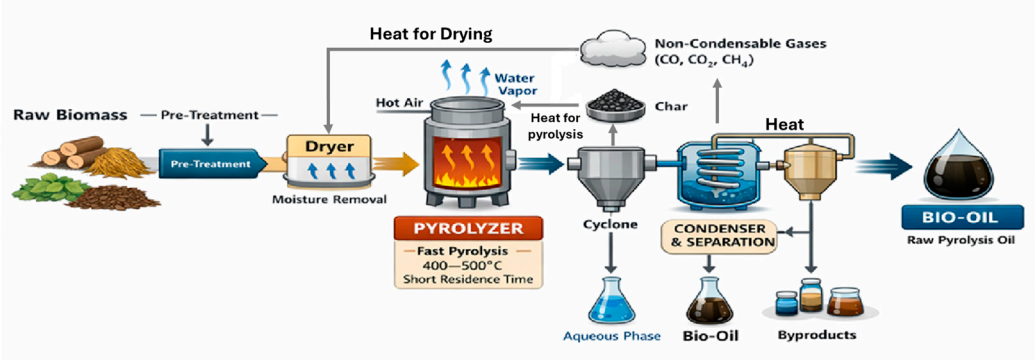

Figure 5. Process flow diagram of a fast-pyrolysis biorefinery showing biomass preparation, reactor, vapour condensation, char/gas combustor, steam and electricity export.

Staged and fractionating concepts are gaining prominence. Two-stage pyrolysis, where an initial low-temperature step is followed by a higher-temperature cracking stage, offers temporal control over primary and secondary reactions. Py-GC/MS and online MS studies show that early vapour fractions are enriched in organic acids and light oxygenates, while later fractions contain more phenolics and aromatics—effectively fractionating the oil into families that can be routed to different upgrading or product lines. This kind of fractionation can be represented schematically in Figures 1 and 4.

Catalytic fast pyrolysis and catalytic co-pyrolysis have been intensely studied in micro-pyrolyser and pilot setups. Zeolites such as HZSM-5 and related MFI structures are particularly effective at reducing oxygen content and generating monocyclic aromatics, though often at the cost of increased coke formation and catalyst deactivation. Hierarchical and mesoporous variants can alleviate diffusion limitations and shift selectivity towards lighter aromatics. Plasma-assisted stages downstream of catalytic pyrolysis have been used to further tune vapour composition, exemplifying the trend towards process intensification.

The common thread across these reactor concepts is the tight coupling between design choices and analytical feedback. Without the detailed product maps discussed in Section 4, it would be impossible to assess whether a given intensification step genuinely improves the fuel or material value of the outputs.

6. Energy Utilisation Pathways

6.1. Fast-Pyrolysis Biorefineries and Polygeneration

Commercial fast-pyrolysis plants processing tens of megawatts of dry biomass now exist and provide valuable performance benchmarks. Figure 5 shows a simplified three-platform biorefinery based on a 25 MW_th fluidised-bed system: biomass is dried and fed to a fast-pyrolysis reactor; vapours are rapidly quenched to produce fast-pyrolysis bio-oil (FPBO); char and non-condensable gases are combusted to supply process heat, drive a steam cycle and sometimes export electricity [75–78].

Typical metrics for such a plant include FPBO output on the order of 20–25 kt per year from roughly 50 kt per year of dry woody residues, net useful-energy efficiency (FPBO + steam + electricity) around 85–86%, and cradle-to-gate FPBO emissions of a few kg CO_2-equivalent per GJ of fuel. Life-cycle assessments indicate substantial greenhouse-gas reductions compared with fossil heating oil when FPBO displaces industrial heat [41,76,79–81].

Table 4 places these numbers alongside those for slow-pyrolysis biochar systems and indirect gasification, providing a concise comparison of energy and environmental indicators [24,76,79–83].

Table 4. A comparison of TEA/LCA indicators for three archetypal systems.

Slow Pyrolysis Biochar Plant	Fast-Pyrolysis Biorefinery	Indirect Gasification via FPBO (Fast-Pyrolysis Bio-Oil)
Technical Biochar yield (wt%) Biochar energy efficiency (%) Net electric efficiency (%) Total energy recovery efficiency (%)	**Technical** Feedstock type and plant capacity Plant life Product Yields and Energy Efficiencies	**Technical** Feedstock type & plant capacity Plant life Product Yields and Energy Efficiencies
Economic CAPEX OPEX Levelised Cost of Biochar (£/t) Cost per tCO_2 removed	**Economic** CAPEX OPEX Product value Payback period	**Economic** CAPEX included an air separation unit OPEX Product value Payback period
Environmental (LCA) GWP ($kgCO_2$-eq/t feedstock) Net CO_2 removed (tCO_2/t) Carbon removal efficiency (%)	**Environmental (LCA)** Global warming potential (GWP) Net CO_2 avoided Fossil energy demand	**Environmental (LCA)** Net CO_2 removed (tCO_2/t) Carbon removal efficiency (%)
[84]	[85]	[86]

6.2. Bio-Oil in Combustion and Refining Systems

From an energy-system perspective, FPBO can be burned directly in suitably adapted boilers and furnaces, co-fired with fossil fuels, co-processed in refinery units such as FCC and hydrotreaters, or used as a chemical feedstock for resins, solvents, acids and bitumen modifiers. Direct use typically requires burner and material adaptations due to acidity, viscosity and low stability. Co-processing in refineries mitigates some of these issues but raises questions about long-term catalyst performance and integration with existing process control strategies [77,78,87–89]. Catalytic fast pyrolysis aims to embed part of the upgrading in the vapour phase itself, front-loading the deoxygenation task.

Figure 4 can be used to illustrate the shift from a raw to an upgraded oil: a reduction in light acids and carbonyls, an increase in hydrocarbons and a contraction of the "heavy tail" of oligomeric species [30,32–36,90]. These shifts must be balanced against hydrogen consumption, coke formation and equipment complexity [73,87–90].

6.3. Pyrolysis Gas and Syngas-Based Routes

The gas fraction underpins process energy self-sufficiency and offers additional options for power and syngas production. Table 2 summarises representative compositions and heating values. In many slow- or intermediate-pyrolysis units, the gas, perhaps supplemented with part of the char, is sufficient to maintain reactor temperature and run ancillary equipment, with surplus available for a small engine or ORC.

Comparative studies using process simulation show that, in terms of energy and exergy efficiency, direct gasification of solid biomass generally outperforms indirect routes via fast-pyrolysis oil. Figure 6 contrasts these pathways. At typical gasification conditions, direct gasification may achieve energy and exergy efficiencies in the low-60% range, compared with somewhat lower values for the FPBO route. The latter, however, offers the logistical advantage of transporting an energy-dense liquid rather than bulky solids, potentially enabling different plant siting and feedstock-supply configurations.

By-product recycling concepts close some loops. Biochar and heavy oil fractions can act as internal sorbents and catalysts for tar removal and gas cleanup, with spent sorbents ultimately returned to the combustor or gasifier for energy recovery. This reduces external reagent demand and aligns with circular-economy narratives.

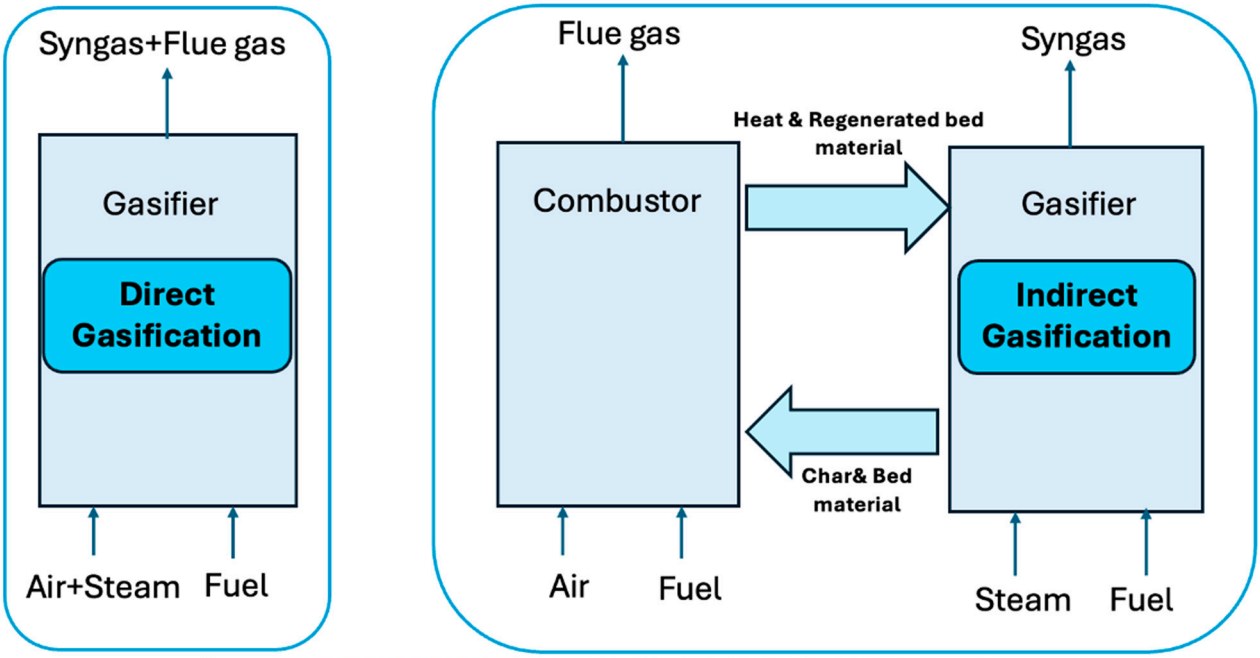

Energy Efficiency	**Direct** > Indirect
Exergy Efficiency	**Direct** > Indirect
CO2 Emission Intensity	Direct < **Indirect**
DME Unit Cost	Direct < **Indirect**

Figure 6. Two typical gasification conditions, direct and indirect pathways.

6.4. Biochar as an Energy Vector and Carbon-Removal Tool

Biochar can be used as a solid fuel, a soil amendment, an adsorbent, a construction material or a precursor for high-value carbons [20,24–27,65–68,71]. From an energy perspective, char heating values of 24–31 MJ kg^{-1} are typical for chars produced from lignocellulosic biomass at 400–600 °C, often exceeding the parent biomass HHV by 20–50%. From a climate perspective, biochar offers a route to relatively durable carbon storage, especially when H/C_org and O/C criteria indicate high aromaticity and low reactivity [20,24,41,65–68,91].

Economic analyses of slow-pyrolysis systems suggest that when co-produced heat and power are valued, biochar minimum selling prices in the tens to low hundreds of dollars per tonne are feasible, competitive with some fossil carbons and with meaningful carbon-removal potential. Life-cycle assessments of biochar systems typically report net negative emissions per tonne of dry feedstock, provided that residues are used and that char stability is high [41,79–82]. Table 4 includes indicative economic and environmental metrics for such systems. Field data on long-term stability and agronomic performance are still emerging and heterogeneous, which is one reason why certification schemes and carbon-credit methodologies emphasise both rigorous characterisation and conservative accounting rules [41,65–68,79–81].

7. Modelling, Optimisation and Digital Tools

Modelling in biomass pyrolysis now spans detailed kinetic schemes, CFD-based reactor simulations, process-flowsheet models and purely data-driven surrogates.

Kinetic and reactor-scale models, often anchored to TGA and micro-pyrolyser data, resolve the interplay of heat transfer, devolatilisation, secondary cracking and hydrodynamics, especially in fluidised beds and augers. Process models built in general-purpose simulators, then integrate these reactor blocks into larger systems that may include drying, gasification, Fischer–Tropsch synthesis or refinery units [24,36,73,76–78,83].

On the data-driven side, models such as ANFIS, random forests and support vector machines have been used to predict yields, heating values and stability metrics from feedstock and process variables [33,40,75,92–94]. Table 3 summarises representative modelling and ML studies, listing their methods, input features, outputs and performance. Li and co-workers showed that GA- and PSO-optimised ANFIS architectures can outperform conventional regressions for bio-oil yield prediction, while Zhu and others demonstrated similar gains for biochar yield and carbon content prediction. Yin and co-workers' TGA + SVM approach illustrates a classification-oriented use case, where the objective is feedstock identification rather than yield prediction. More recent work has applied ML directly to predict bio-oil properties and biochar stability from compositional and process descriptors.

Figure 7 sketches a generic ML workflow for pyrolysis optimisation: compositional data, TGA curves and process conditions feed ML models, which output predicted yields and properties. These predictions can in turn feed into techno-economic and life-cycle models, enabling multi-objective optimisation over both engineering and environmental criteria [76–83].

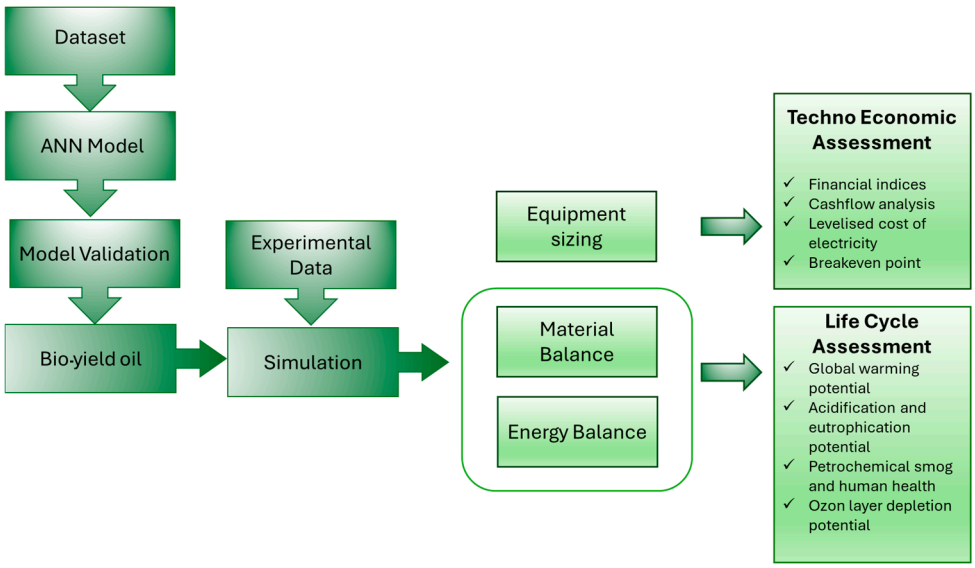

Figure 7. Generic ML workflow for pyrolysis optimisation.

8. Techno-Economic and Environmental Assessment

Techno-economic analysis and life-cycle assessment have become standard components of serious pyrolysis studies [20,21,24,34,41,76–83,92].

For fast-pyrolysis biorefineries, TEA typically evaluates capital and operating costs for biomass preparation, reactor and separation sections, utilities and upgrading, alongside revenues from FPBO, steam and electricity [75–78,83]. In a 25 MW_th reference case, total annualised costs and revenues are of similar magnitude, with profitability strongly sensitive to feedstock cost and FPBO selling price [75–78,83]. LCA results indicate substantial greenhouse-gas reductions compared with fossil heat, often in the range of 80–96% on an energy-equivalent basis [41,76,79–81].

For slow-pyrolysis and biochar-oriented systems, TEA must consider additional revenue streams such as carbon-removal credits, soil-improvement benefits and specialty-

carbon markets [20,24,41,65–68,82]. LCAs for such systems often report net negative emissions per tonne of dry feedstock, provided that residues are used and that char stability is high [41,79–82].

Table 4 compares TEA/LCA indicators for three archetypal systems: (i) a fast-pyrolysis biorefinery focused on FPBO and process steam; (ii) a slow-pyrolysis plant optimised for biochar and heat; and (iii) an indirect gasification route where biomass is first converted to FPBO and then to syngas [24,76–83]. Indicators include overall energy efficiency, specific GHG emissions, indicative cost metrics and dominant sensitivities. Allocation choices (how to distribute burdens among oil, char, gas, steam and electricity) and stability assumptions for biochar remain contentious, and should be made explicit in any study [79–82].

9. Conclusions

The last decade has seen biomass pyrolysis move from proof-of-concept towards technically and economically credible deployment in several niches. The quality and depth of characterisation work now available—on feedstocks, intermediates and products—make it possible to design pyrolysis systems around specific energy and material functions rather than treating them as generic "bio-oil factories" [1–4,6–8,10–14,27–30].

Several conclusions stand out. First, feedstock composition and process conditions jointly define a high-dimensional product space; neither can be treated as a minor perturbation on the other [21,22,25–28,33,39,42,75,92]. Second, advanced analytical methods, especially for bio-oil and biochar, have become integral to process design and catalyst development, not optional extras [29,30,32–37,65–68]. Third, machine-learning models, when used judiciously, complement mechanistic understanding and enable rapid exploration and optimisation over complex variable spaces [33,40,68,75,92,94]. Finally, at the system level, both fast- and slow-pyrolysis configurations can achieve high energy efficiencies and compelling greenhouse-gas performance, particularly when residues are used and carbon storage is correctly valued [20,21,24,41,76–83,95,96].

Remaining challenges include standardisation of characterisation protocols, long-term field validation of biochar performance, robust integration with existing refineries and power systems, and careful techno-economic analysis and life-cycle assessment under realistic policy and market conditions. Addressing these will determine whether pyrolysis becomes a core pillar of low-carbon energy and carbon-removal strategies or remains confined to specialised niches.

Author Contributions: Conceptualisation, H.R.N.; methodology, H.R.N.; investigation, H.R.N. and M.N.G.; resources, H.R.N.; data curation, M.N.G.; writing—original draft preparation, H.R.N. and M.N.G.; writing—review and editing, H.R.N.; visualisation, M.N.G.; supervision, H.R.N.; project administration, H.R.N. All authors have read and agreed to the published version of the manuscript.

Funding: This research received no external funding.

Data Availability Statement: No new data were created or analysed in this study. Data sharing is not applicable to this article.

Acknowledgments: The authors gratefully acknowledge the School of Engineering and Computing at the University of Lancashire for institutional support. The authors also thank the anonymous reviewers and the Academic Editor for their constructive comments, which helped improve the clarity and focus of the manuscript.

Conflicts of Interest: The authors declare no conflicts of interest.

Abbreviations

- "higher heating value (HHV)"
- "lower heating value (LHV)"
- "temperature–vacuum swing adsorption (TVSA)"
- "carbon capture, utilisation and storage (CCUS)"
- "thermogravimetric analysis (TGA)" and "derivative thermogravimetry (DTG)"
- "techno-economic analysis (TEA)" and "life-cycle assessment (LCA)"
- "fast-pyrolysis bio-oil (FPBO)"

References

1. Vardian, M.; Nasriani, H.R.; Faghihi, R.; Vardian, A.; Jowkar, S. Porosity and permeability prediction from well logs using an adaptive neuro-fuzzy inference system in a naturally fractured gas-condensate reservoir. *Energy Sources Part A Recovery Util. Environ. Eff.* **2016**, *38*, 435–441. https://doi.org/10.1080/15567036.2011.592923.
2. Nasriani, H.R.; Kalantariasl, A. Choke performance in high-rate gas condensate wells under subcritical flow condition. *Energy Sources Part A Recovery Util. Environ. Eff.* **2015**, *37*, 192–199. https://doi.org/10.1080/15567036.2011.582607.
3. Nasriani, H.R.; Asadi, E.; Nasiri, M.; Khajenoori, L.; Masihi, M. Challenges of fluid phase behavior modeling in Iranian retrograde gas condensate reservoirs. *Energy Sources Part A Recovery Util. Environ. Eff.* **2015**, *37*, 663–669. https://doi.org/10.1080/15567036.2011.594865.
4. Nasriani, H.R.; Jamiolahmady, M. Maximizing fracture productivity in unconventional fields; analysis of post hydraulic fracturing flowback cleanup. *J. Nat. Gas Sci. Eng.* **2018**, *52*, 529–548. https://doi.org/10.1016/j.jngse.2018.01.045.
5. Nasriani, H.R.; Jamiolahmady, M.; Saif, T.; Sánchez, J. A systematic investigation into the flowback cleanup of hydraulic-fractured wells in unconventional gas plays. *Int. J. Coal Geol.* **2018**, *193*, 46–60. https://doi.org/10.1016/j.coal.2018.04.012.
6. Nasriani, H.R.; Jamiolahmady, M. Flowback cleanup mechanisms of post-hydraulic fracturing in unconventional natural gas reservoirs. *J. Nat. Gas Sci. Eng.* **2019**, *66*, 316–342. https://doi.org/10.1016/j.jngse.2019.04.006.
7. Nasriani, H.; Jamiolahmady, M. Optimising Flowback Strategies in Unconventional Reservoirs: The Critical Role of Capillary Forces and Fluid Dynamics. *Energies* **2024**, *17*, 5822. https://doi.org/10.3390/en17235822.
8. Nasriani, H.R.; Jamiolahmady, M. Permeability Jailbreak: A Deep Simulation Study of Hydraulic Fracture Cleanup in Heterogeneous Tight Gas Reservoirs. *Energies* **2025**, *18*, 3618. https://doi.org/10.3390/en18143618.
9. Medaiyese, F.J.; Nasriani, H.R.; Khajenoori, L.; Khan, K.; Badiei, A. From Waste to Energy: Enhancing Fuel and Hydrogen Production through Pyrolysis and In-Line Reforming of Plastic Wastes. *Sustainability* **2024**, *16*, 4973. https://doi.org/10.3390/su16124973.
10. Joonaki, E.; Rostaminikoo, E.; Ghanaatian, S.; Nasriani, H. Thermodynamics of Hydrogen; Analysing and Refining of Critical Flow Factor Through Comprehensive Uncertainty Assessment and Experimental Data Integration. *Abu Dhabi Int. Pet. Exhib. Conf.* **2024**, D031S107R003. https://doi.org/10.2118/222973-MS.
11. Rostaminikoo, E.; Ghanaatian, S.; Joonaki, E.; Nasriani, H.R.; Whitton, J. Advanced thermodynamics of hydrogen and natural gas blends for gas transmission and distribution networks. *Meas. Sens.* **2025**, *38*, 101765. https://doi.org/10.1016/j.measen.2024.101765.
12. Joonaki, E.; Rostaminikoo, E.; Ghanaatian, S.; Nasriani, H.R. Thermodynamic properties of hydrogen containing systems and calculation of gas critical flow factor. *Meas. Sens.* **2025**, *38*, 101587. https://doi.org/10.1016/j.measen.2024.101587.
13. Gholami, S.; Rostaminikoo, E.; Khajenoori, L.; Nasriani, H.R. Density determination of CO_2-Rich fluids within CCUS processes. *Meas. Sens.* **2025**, *38*, 101739. https://doi.org/10.1016/j.measen.2024.101739.
14. Medaiyese, F.J.; Nasriani, H.R.; Khan, K.; Khajenoori, L. Sustainable hydrogen production from plastic waste: Optimizing pyrolysis for a circular economy. *Hydrogen* **2025**, *6*, 15. https://doi.org/10.3390/hydrogen6010015.
15. Ghiri, M.N.; Nasriani, H.R.; Khajenoori, L.; Mohammadkhani, S.; Williams, K.S. Dynamic Temperature–Vacuum Swing Adsorption for Sustainable Direct Air Capture: Parametric Optimisation for High-Purity CO_2 Removal. *Sustainability* **2025**, *17*, 6796. https://doi.org/10.3390/su17156796.
16. Gandomkar, A.; Torabi, F.; Nasriani, H.R.; Enick, R.M. Maximising CO_2 sequestration efficiency in deep saline aquifers through in-situ generation of CO_2-in-brine foam incorporating novel CO_2-soluble non-ionic surfactants. *Chem. Eng. J.* **2025**, *521*, 166102. https://doi.org/10.1016/j.cej.2025.166102.

17. Ghiri, M.N.; Nasriani, H.R.; Khajehnoori, L.; Williams, K.S.; Khani, S.M.; Rostaminikoo, E. Multi-Objective Optimization of CO_2 Capture from Ambient Air via TVSA Process Modeling. *World CCUS Conf.* **2025**, *2025*, 1–5. https://doi.org/10.3997/2214-4609.202522131.
18. Nasiri-ghiri, M.; Nasriani, H.R.; Khajenoori, L.; Rasmussen, S.K.; Williams, K. Surrogate-assisted cyclic performance optimisation of direct air capture using amine-functionalised metal–organic frameworks. *Sep. Purif. Technol.* **2025**, *383*, 136177. https://doi.org/10.1016/j.seppur.2025.136177.
19. Medaiyese, F.J.; Nasiri-Ghiri, M.; Nasriani, H.R.; Khajenoori, L.; Khan, K. Pinch-guided heat integration for hydrogen production from mixed plastic waste. *Hydrogen* **2026**, *17*, 38. https://doi.org/10.3390/hydrogen7010038.
20. Laird, D.A.; Brown, R.C.; Amonette, J.E.; Lehmann, J. Review of the pyrolysis platform for coproducing bio-oil and biochar. *Biofuels Bioprod. Bioref.* **2009**, *3*, 547–562. https://doi.org/10.1002/bbb.169.
21. Bridgwater, A.V. Review of fast pyrolysis of biomass and product upgrading. *Biomass Bioenergy* **2012**, *38*, 68–94. https://doi.org/10.1016/j.biombioe.2011.01.048.
22. Bridgwater, A.V.; Meier, D.; Radlein, D. An overview of fast pyrolysis of biomass. *Org. Geochem.* **1999**, *30*, 1479–1493.
23. Mohan, D.; Pittman, C.U.; Steele, P.H. Pyrolysis of wood/biomass for bio-oil: A critical review. *Energy Fuels* **2006**, *20*, 848–889. https://doi.org/10.1021/ef0502397.
24. Czernik, S.; Bridgwater, A.V. Overview of applications of biomass fast pyrolysis oil. *Energy Fuels* **2004**, *18*, 590–598. https://doi.org/10.1021/ef034067u.
25. Dhyani, V.; Bhaskar, T. A comprehensive review on the pyrolysis of lignocellulosic biomass. *Renew. Sustain. Energy Rev.* **2018**, *81*, 1350–1371. https://doi.org/10.1016/j.renene.2017.04.035.
26. Tripathi, M.; Sahu, J.N.; Ganesan, P. Effect of process parameters on production of biochar from biomass waste through pyrolysis: A review. *Renew. Sustain. Energy Rev.* **2016**, *55*, 467–481. https://doi.org/10.1016/j.rser.2015.10.122.
27. Sharma, A.; Pareek, V.; Zhang, D. Biomass pyrolysis—A review of modelling, process parameters and catalytic studies. *Renew. Sustain. Energy Rev.* **2015**, *50*, 1081–1096. https://doi.org/10.1016/j.rser.2015.04.193.
28. Yang, H.; Yan, R.; Chen, H.; Zheng, C.; Lee, D.H.; Liang, D.T. In-depth investigation of biomass pyrolysis based on three major components: Hemicellulose, cellulose and lignin. *Energy Fuels* **2006**, *20*, 388–393. https://doi.org/10.1021/ef0580117.
29. Stefanidis, S.D.; Kalogiannis, K.G.; Iliopoulou, E.F.; Michailof, C.M.; Pilavachi, P.A.; Lappas, A.A. A study of lignocellulosic biomass pyrolysis via the pyrolysis of cellulose, hemicellulose and lignin. *J. Anal. Appl. Pyrolysis* **2014**, *105*, 143–150. https://doi.org/10.1016/j.jaap.2013.10.013.
30. Di Blasi, C. Modeling chemical and physical processes of wood and biomass pyrolysis. *Prog. Energy Combust. Sci.* **2008**, *34*, 47–90. https://doi.org/10.1016/j.pecs.2006.12.001.
31. Bridgwater, A.V. Biomass fast pyrolysis. *Therm. Sci.* **2004**, *16*, 679–702. https://doi.org/10.2298/TSCI0402021B.
32. Demirbas, A. Effects of temperature and particle size on bio-char yield from pyrolysis of agricultural residues. *J. Anal. Appl. Pyrolysis* **2004**, *72*, 243–248. https://doi.org/10.1016/j.jaap.2004.07.003.
33. Altıkat, A.; Alma, M.H.; Altıkat, A.; Bilgili, M.E.; Altıkat, S. A comprehensive study of biochar yield and quality concerning pyrolysis conditions: A multifaceted approach. *Sustainability* **2024**, *16*, 937.
34. Vilas-Boas, A.C.; Tarelho, L.A.; Oliveira, H.S.; Silva, F.G.; Pio, D.T.; Matos, M.A. Valorisation of residual biomass by pyrolysis: Influence of process conditions on products. *Sustain. Energy Fuels* **2024**, *8*, 379–396.
35. Zhou, Z.; Zhu, L.; Cui, C.; Liu, H.; Shen, Y.; Yuan, W.; Qi, F. Pyrolysis of lignocellulosic biomass: Molecular-level insights with online ultrahigh-resolution mass spectrometry. *Fuel Process. Technol.* **2022**, *236*, 107439.
36. Liu, P.; Zhuang, H.; Qian, Y.; Yang, J.; Pan, Y.; Zhou, Z.; Jia, L.; Qi, F. Recent advances in mass spectrometric studies on the reaction process of biomass pyrolysis. *Fuel Process. Technol.* **2022**, *237*, 107473.
37. Staš, M.; Kubička, D.; Chudoba, J.; Pospisil, M. Overview of analytical methods used for chemical characterization of pyrolysis bio-oil. *Energy Fuels* **2014**, *28*, 385–402.
38. Lazzari, E.; Schena, T.; Marcelo, M.C.; Primaz, C.T.; Silva, A.N.; Ferrao, M.F.; Bjerk, T.; Caramao, E.B. Classification of biomass through their pyrolytic bio-oil composition using FTIR and PCA analysis. *Ind. Crops Prod.* **2018**, *111*, 856–864.
39. Biagini, E.; Tognotti, L. A generalized procedure for the devolatilisation of biomass fuels based on the chemical components. *Energy Fuels* **2014**, *28*, 614–623. https://doi.org/10.1021/ef402139v.
40. Yin, C.; Deng, X.; Yu, Z.; Liu, Z.; Zhong, H.; Chen, R.; Cai, G.; Zheng, Q.; Liu, X.; Zhong, J.; et al. Auto-classification of biomass through characterization of their pyrolysis behaviors using thermogravimetric analysis with support vector machine algorithm: Case study for tobacco. *Biotechnol. Biofuels* **2021**, *14*, 106.

41. Woolf, D.; Amonette, J.E.; Street-Perrott, F.A.; Lehmann, J.; Joseph, S. Sustainable biochar to mitigate global climate change. *Nat. Commun.* **2010**, *1*, 56. https://doi.org/10.1038/ncomms1053.
42. Kan, T.; Strezov, V.; Evans, T.J. Lignocellulosic biomass pyrolysis: A review of product properties and effects of pyrolysis parameters. *Renew. Sustain. Energy Rev.* **2016**, *57*, 1126–1140. https://doi.org/10.1016/j.rser.2015.12.185.
43. Talwar, P.; Agudelo, M.A.; Nanda, S. Pyrolysis process, reactors, products, and applications: A review. *Energies* **2025**, *18*, 2979.
44. Pattiya, A.; Suttibak, S. Fast pyrolysis of sugarcane residues in a fluidised bed reactor with a hot vapour filter. *J. Energy Inst.* **2017**, *90*, 110–119.
45. Butler, E.; Devlin, G.; Meier, D.; McDonnell, K. A review of recent laboratory research and commercial developments in fast pyrolysis and upgrading. *Renew. Sustain. Energy Rev.* **2011**, *15*, 4171–4186. https://doi.org/10.1016/j.rser.2011.07.035.
46. Awad, M.I.; Makkawi, Y.; Hassan, N.M. Yield and energy modeling for biochar and bio-oil using pyrolysis temperature and biomass constituents. *ACS Omega* **2024**, *9*, 18654–18667. https://doi.org/10.1021/acsomega.4c01646.
47. Mariyam, S.; Alherbawi, M.; McKay, G.; Al-Ansari, T. A predictive model for biomass waste pyrolysis yield: Exploring the correlation of proximate analysis and product composition. *Energy Convers. Manag. X* **2025**, *25*, 100831.
48. Singh, Y.; Singh, N.K.; Sharma, A.; Lim, W.H.; Palamanit, A.; Alhussan, A.A.; El-kenawy, E.S. Bio-oil yield maximization and characteristics of neem based biomass at optimum conditions along with feasibility of biochar through pyrolysis. *AIP Adv.* **2024**, *14*, 085104.
49. Maneechakr, P.; Karnjanakom, S. Improving the bio-oil quality via effective pyrolysis/deoxygenation of palm kernel cake over a metal (Cu, Ni, or Fe)-doped carbon catalyst. *ACS Omega* **2021**, *6*, 20006–20014.
50. Madhu, P.; Vidhya, L.; Vinodha, S.; Wilson, S.; Sekar, S.; Patil, P.P.; Kaliappan, S.; Prabhakar, S. Co-pyrolysis of Hardwood Combined with Industrial Pressed Oil Cake and Agricultural Residues for Enhanced Bio-Oil Production. *J. Chem.* **2022**, *2022*, 9884766.
51. Mulimani, H.V.; Navindgi, M.C. High calorific value fuel from pyrolysis of waste de-oiled seed cakes. *Nat. Environ. Pollut. Technol.* **2018**, *17*, 807–813.
52. Jerzak, W.; Reinmöller, M.; Magdziarz, A. Estimation of the heat required for intermediate pyrolysis of biomass. *Clean Technol. Environ. Policy* **2022**, *24*, 3061–3075.
53. Tinwala, F.; Mohanty, P.; Parmar, S.; Patel, A.; Pant, K.K. Intermediate pyrolysis of agro-industrial biomasses in bench-scale pyrolyser: Product yields and its characterization. *Bioresour. Technol.* **2015**, *188*, 258–264.
54. Ahmed, A.; Yub Harun, N.; Waqas, S.; Arshad, U.; Ghalib, S.A. Optimization of operational parameters using artificial neural network and support vector machine for bio-oil extracted from rice husk. *ACS Omega* **2024**, *9*, 26540–26548.
55. Ramajayam, J.G.; Samal, P.; Lakshmipathy, M.V.; Perumal, T.; Govindarajan, M.; Baidya, T.; Yadav, K.K.; Bhutto, J.K.; Alreshidi, M.A.; Hakami, H. Emerging Roles of Ionic Liquids in Biodiesel: A Review on Catalysis, Process Design, and Recyclability. *Energy Fuels* **2025**, *39*, 15961–15990. https://doi.org/10.1021/acs.energyfuels.5c02309.
56. Kandpal, S.; Tagade, A.; Sawarkar, A.N. Critical insights into ensemble learning with decision trees for the prediction of biochar yield and higher heating value from pyrolysis of biomass. *Bioresour. Technol.* **2024**, *411*, 131321.
57. Mathur, J.; Baruah, B.; Tiwari, P. Prediction of bio-oil yield during pyrolysis of lignocellulosic biomass using machine learning algorithms. *Can. J. Chem. Eng.* **2023**, *101*, 2457–2471.
58. Mafat, I.H.; Palla, S.; Ambati, S.R.; Narayana, R.; Kumar, K.V.; Swaroop, G.J. Data-driven modeling of bio-oil yield in agricultural biomass pyrolysis with machine learning. *Int. J. Hydrogen Energy* **2024**, *137*, 1248–1259.
59. Tian, H.; Zou, Y.; Cheng, S.; Lv, D.; Wang, Z.; Huang, Z.; Fu, J. Machine learning based prediction of nitrogenous product yield in biomass pyrolysis oil. *J. Energy Inst.* **2025**, *123*, 102291.
60. Bi, D.; Wang, H.; Liu, Y.; Qin, Z.; Song, X.; Liu, S. Machine learning-based prediction model for the yield of nitrogen-enriched biomass pyrolysis products: Performance evaluation and interpretability analysis. *J. Anal. Appl. Pyrolysis* **2024**, *182*, 106723.
61. Timilsina, M.S.; Chaudhary, Y.; Bhattarai, P.; Uprety, B.; Khatiwada, D. Optimizing pyrolysis and Co-Pyrolysis of plastic and biomass using Artificial Intelligence. *Energy Convers. Manag. X* **2024**, *24*, 100783.
62. Cheenkachorn, K.; Prapainainar, C.; Wijakmatee, T. Machine learning-driven modeling of biomass pyrolysis product distribution through thermal parameter sensitivity. *Renew. Energy* **2025**, *248*, 123108.
63. Sakheta, A.; Raj, T.; Nayak, R.; O'Hara, I.; Ramirez, J.A. Development and assessment of hybrid machine learning model of biomass pyrolysis process. *Chem. Eng. Sci.* **2025**, *310*, 121552.
64. Jia, L.; Shao, W.; Wang, J.; Qian, Y.; Chen, Y.; Yang, Q. Machine learning-aided prediction of bio-BTX and olefins production from zeolite-catalyzed biomass pyrolysis. *Energy* **2024**, *306*, 132478.

65. Ahmad, M.; Rajapaksha, A.U.; Lim, J.E.; Zhang, M.; Bolan, N.; Mohan, D.; Vithanage, M.; Lee, S.S.; Ok, Y.S. Biochar as a sorbent for contaminant management in soil and water: A review. *Chemosphere* **2014**, *99*, 19–33.
66. Lehmann, J.; Joseph, S. (Eds.) *Biochar for Environmental Management: Science, Technology and Implementation*, Taylor & Francis: Oxfordshire, UK, 2024.
67. Qiu, M.; Liu, L.; Ling, Q.; Cai, Y.; Yu, S.; Wang, S.; Fu, D.; Hu, B.; Wang, X. Biochar for the removal of contaminants from soil and water: A review. *Biochar* **2022**, *4*, 19.
68. Leng, L.; Huang, H.; Li, H.; Li, J.; Zhou, W. Biochar stability assessment methods: A review. *Sci. Total Environ.* **2019**, *647*, 210–222.
69. Biswas, B.; Balla, P.; Krishna, B.B.; Adhikari, S.; Bhaskar, T. Physiochemical characteristics of bio-char derived from pyrolysis of rice straw under different temperatures. *Biomass Convers. Biorefin.* **2024**, *14*, 12775–12783.
70. Nguyen, L.X.; Do, P.T.; Nguyen, C.H.; Kose, R.; Okayama, T.; Pham, T.N.; Miyanishi, T. Properties of Biochars prepared from local biomass in the Mekong Delta, Vietnam. *BioResources* **2018**, *13*, 7325–7344.
71. Qambrani, N.A.; Rahman, M.M.; Won, S.; Shim, S.; Ra, C. Biochar properties and eco-friendly applications for climate change mitigation, waste management, and wastewater treatment: A review. *Renew. Sustain. Energy Rev.* **2017**, *79*, 255–273.
72. Hilten, R.N.; Das, K.C. Comparison of three accelerated aging procedures to estimate bio-oil stability. *Fuel* **2010**, *89*, 2741–2749. https://doi.org/10.1016/j.fuel.2010.03.033.
73. Venderbosch, R.H.; Prins, W. Fast pyrolysis technology development. *Biofuels Bioprod. Bioref.* **2010**, *4*, 178–208. https://doi.org/10.1002/bbb.205.
74. Park, J.Y.; Kim, J.K.; Oh, C.H.; Park, J.W.; Kwon, E.E. Production of bio-oil from fast pyrolysis of biomass using a pilot-scale circulating fluidized bed reactor and its characterization. *J. Environ. Manag.* **2019**, *234*, 138–144.
75. Li, Z.; Zhao, D.; Han, L.; Yu, L.; Jafari, M.M.M. Improved estimation of bio-oil yield based on pyrolysis conditions and biomass compositions using GA- and PSO-ANFIS models. *Biomed. Res. Int.* **2021**, *2021*, 2204021. https://doi.org/10.1155/2021/2204021.
76. Furusjö, E.; Jafri, Y.; Wetterlund–Bio4Energy, E.; Anheden, M.; Kulander, I.; Bioeconomy, J.W. *Techno-Economics of Long and Short Term Technology Pathways for Renewable Transportation Fuel Production*; f3 The Swedish Knowledge Centre for Renewable Transportation Fuels: Gothenburg, Sweden, 2017.
77. Jones, S.B.; Valkenburt, C.; Walton, C.W.; Elliott, D.C.; Holladay, J.E.; Stevens, D.J.; Kinchin, C.; Czernik, S. *Production of Gasoline and Diesel from Biomass via Fast Pyrolysis, Hydrotreating and Hydrocracking: A Design Case*; Pacific Northwest National Laboratory (PNNL): Richland, WA, USA, 2009.
78. Wright, M.M.; Brown, R.C.; Boateng, A.A. Distributed processing of biomass to bio-oil for subsequent production of Fischer–Tropsch liquids. *Biofuels Bioprod. Bioref.* **2008**, *2*, 229–238. https://doi.org/10.1002/bbb.73.
79. Gaunt, J.L.; Lehmann, J. Energy balance and emissions associated with biochar sequestration and pyrolysis bioenergy production. *Environ. Sci. Technol.* **2008**, *42*, 4152–4158. https://doi.org/10.1021/es071361i.
80. Roberts, K.G.; Gloy, B.A.; Joseph, S.; Scott, N.R.; Lehmann, J. Life cycle assessment of biochar systems: Estimating the climate-change potential. *Environ. Sci. Technol.* **2010**, *44*, 827–833. https://doi.org/10.1021/es902266r.
81. Woolf, D.; Lehmann, J.; Lee, D.R. Optimal bioenergy power generation for climate change mitigation with or without carbon sequestration. *Nat. Commun.* **2016**, *7*, 13160. https://doi.org/10.1038/ncomms13160.
82. Brown, T.R.; Wright, M.M.; Brown, R.C. Estimating profitability of two biochar production scenarios: Slow pyrolysis vs. fast pyrolysis. *Biofuels Bioprod. Bioref.* **2011**, *5*, 54–68. https://doi.org/10.1002/bbb.254.
83. Wright, M.M.; Daugaard, D.E.; Satrio, J.A.; Brown, R.C. Techno-economic analysis of biomass fast pyrolysis to transportation fuels. *Fuel* **2011**, *89*, S2–S10. https://doi.org/10.1016/j.fuel.2010.07.029.
84. Bahiri, I.; Ibrahim, M.M.; Zaabout, A. Mapping techno-economic prospects of biochar production through biomass waste pyrolysis pathway. *Energy Convers. Manag.* **2025**, *327*, 119526.
85. Li, Q.; Zhang, Y.; Hu, G. Techno-economic analysis of advanced biofuel production based on bio-oil gasification. *Bioresour. Technol.* **2015**, *191*, 88–96.
86. Zhang, Y.; Brown, T.R.; Hu, G.; Brown, R.C. Comparative techno-economic analysis of biohydrogen production via bio-oil gasification and bio-oil reforming. *Biomass Bioenergy* **2013**, *51*, 99–108.
87. Mortensen, P.M.; Grunwaldt, J.-.D.; Jensen, P.A.; Knudsen, K.G.; Jensen, A.D. A review of catalytic upgrading of bio-oil to engine fuels. *Appl. Catal. A* **2011**, *407*, 1–19. https://doi.org/10.1016/j.apcata.2011.08.046.
88. Huber, G.W.; Iborra, S.; Corma, A. Synthesis of transportation fuels from biomass: Chemistry, catalysts, and engineering. *Chem. Rev.* **2006**, *106*, 4044–4098. https://doi.org/10.1021/cr068360d.

89. Srokol, Z.; Bouche, A.G.; Van Estrik, A.; Strik, R.C.; Maschmeyer, T.; Peters, J.A. Hydrothermal upgrading of biomass to biofuel; studies on some monosaccharide model compounds. *Carbohydr. Res.* **2004**, *339*, 1717–1726.
90. Elliott, D.C. Historical developments in hydroprocessing bio-oils. *Energy Fuels* **2007**, *21*, 1792–1815. https://doi.org/10.1021/ef070044u.
91. Fang, Y.; Singh, B.; Singh, B.P. Temperature dependence of biochar stability in soils: A molecular–level perspective. *Sci. Total Environ.* **2014**, *500–501*, 333–340. https://doi.org/10.1016/j.scitotenv.2014.08.008.
92. Zhu, X.; Li, Y.; Wang, X. Machine learning prediction of biochar yield and carbon contents in biochar based on biomass characteristics and pyrolysis conditions. *Bioresour. Technol.* **2019**, *288*, 121527. https://doi.org/10.1016/j.biortech.2019.121527.
93. Zhang, T.; Cao, D.; Feng, X.; Zhu, J.; Lu, X.; Mu, L.; Qian, H. Machine learning prediction of bio-oil characteristics quantitatively relating to biomass compositions and pyrolysis conditions. *Fuel* **2022**, *312*, 122812.
94. Su, G.; Jiang, P. Machine learning models for predicting biochar properties from lignocellulosic biomass torrefaction. *Bioresour. Technol.* **2024**, *399*, 130519.
95. AV Bridgwater, G.V.C. Peacocke. Fast pyrolysis processes for biomass. *Renew. Sustain. Energy Rev.* **2000**, 4, 1–73. https://doi.org/10.1016/S1364-0321(99)00007-6.
96. Zhang, Y.; Liang, Y.; Brindhadevi, K.; Li, S.; Yuan, Y.; Pugazhendhi, A.; Zhang, D.; Xia, C.; Wu, Y.; Xie, H. A review of biomass pyrolysis gas: Forming mechanisms, influencing parameters, and product application upgrades. *Fuel* **2023**, *347*, 128461. https://doi.org/10.1016/j.fuel.2023.128461.